

Daniel C. Fisher¹, David L. Fox¹ & Larry D. Agenbroad²

¹ University of Michigan, Ann Arbor

² Northern Arizona University, Flagstaff

Tusk growth rate and season of death of *Mammuthus columbi* from Hot Springs, South Dakota, USA

Fisher, D.C., Fox, D.L. & Agenbroad, L.D., 2003 - Tusk growth rate and season of death of *Mammuthus columbi* from Hot Springs, South Dakota, USA - in: Reumer, J.W.F., De Vos, J. & Mol, D. (eds.) - ADVANCES IN MAMMOTH RESEARCH (Proceedings of the Second International Mammoth Conference, Rotterdam, May 16-20 1999) - DEINSEA 9: 117-133 [ISSN 0923-9308] Published 24 May 2003

Samples of dentin from the proximal end of mammoth tusks provide information on paleoclimate and tusk growth rate during the last years of life. We have used such data to determine season of death for multiple individuals and to characterize the cycle of seasonal variation in environmental conditions typical for the region of the Mammoth Site of Hot Springs, South Dakota, 26,000 yBP. We document patterns of change in oxygen isotope composition of dentinal hydroxyapatite and in thickness of circaseptan incremental features in tusk dentin. Oxygen isotope profiles show annually repeating patterns with a long autumn-winter phase of declining values and a shorter spring-summer phase of rising values. Tusk growth rate profiles confirm the annual nature of these cycles and, in certain years, the isotope-based interpretation of season. Death seems to have had a bimodal distribution, occurring in a pattern implying elevated risk in autumn and spring. Moreover, death is usually preceded by an interval of reduced seasonal range in oxygen isotope values and of aseasonal (highly variable) patterns of tusk growth. We interpret this as reflecting a period of increased reliance on the isotopically stable water and food resources associated with one or more of the sinkhole-artesian spring systems that formed this site and others like it in the vicinity. Tusks thus record periods both before and after development of this site-fidelity.

Daniel C. Fisher (to whom correspondence should be addressed), Museum of Paleontology, University of Michigan, Ann Arbor, MI 48109-1079 USA, email dcfisher@umich.edu; David L. Fox, (present address) Dept. of Geology & Geophysics, University of Minnesota, Minneapolis, MN 55455-0129 USA: e-mail: dlfox@umn.edu; Larry D. Agenbroad, Department of Geology, Northern Arizona University, Flagstaff, AZ 86011 USA, email Larry.Agenbroad@nau.edu

Keywords: *Mammuthus columbi*, tusk growth, oxygen isotopes, season of death, paleoclimate

INTRODUCTION

Tusks of adult proboscideans are remarkable not only in size and shape, but also in internal structure. Layers of dentin organized as a series of nested cones comprise the principal mass of elephantid tusks and consist of material deposited in a distal-to-proximal sequence, from early in ontogeny to the time of death. Complete tusks thus represent much, if not all, of an animal's lifetime (Sikes 1971). Regular alternations in the conditions of

growth, at several different time scales, can be traced in cross section as a hierarchical system of incremental features (Fisher 1987, 1996, 2001). These structurally distinct laminae also vary in composition, reflecting the interaction of behavioral, physiological, and environmental factors (Koch *et al.* 1989; Fisher & Fox, submitted). Tusk analyses may thus address a wide range of paleobiological and paleoenvironmental questions.

This study focuses on samples of dentin from near the growing end of tusks of *Mammuthus columbi* from the Mammoth Site of Hot Springs, South Dakota, USA. Our observations were designed to assess rates of addition of new dentin to the tusk during the last few years of life and to deduce the season or seasons of year in which death occurred. The goal of this research is to enhance understanding of climate and forage conditions encountered by these animals and to offer insight into circumstances associated with the entrapment and death of the mammoths that comprise this dramatic assemblage. The Hot Springs Mammoth Site preserves the largely disarticulated skeletons of over fifty Columbian mammoths. Geological context and site taphonomy are discussed extensively by Agenbroad (1994a), Laury (1994), and Agenbroad & Mead (1994). Based on these studies, it appears that the assemblage accumulated within a period possibly less than one thousand years and dates to about 26,000 yBP. It represents a unique sample of essentially a single population of Columbian mammoths from a time prior to the Last Glacial Maximum (LGM). As such, it represents an interesting point of comparison with mammoths from nearer the LGM and from the terminal Pleistocene.

The Hot Springs mammoths are mostly young-adult to adult males (Lister & Agenbroad 1994) that fell into a warm, spring-fed pond occupying a steep-walled sinkhole from which they were unable to escape. The younger individuals may have been only recently excluded from their natal matriarchal family unit and may thus have been relatively inexperienced. In addition, males of all ages represented here (Agenbroad 1994b; Lister 1994) would usually have been solitary, by analogy with Recent elephants. Entrapment has been viewed as essentially accidental, with failure to escape largely a function of lack of assistance from conspecifics. The mechanism of entrapment has been interpreted as involving both the steepness of the sinkhole margins and the slippery condi-

tions they could have presented to a large, panicked animal. Agenbroad & Mead (1994: 286) portray the proximate cause of death of entrapped mammoths as either starvation or drowning.

These animals may have been attracted to the sinkhole margin by water and/or food; the warm water inferred to have occupied this setting (Laury 1994), and currently flowing in many of the region's extant artesian springs, could have moderated conditions enough to maintain some access to food and water even in seasons when their availability was limited in the surrounding area (Agenbroad & Mead 1994). If the seasonal distribution of regional scarcity of food and water was the main factor controlling attraction to this site, one might expect a predominance of winter deaths. On the other hand, if mammoths frequented the sinkhole in all seasons, and entrapment was more a consequence of temporally random mis-step or bank collapse, one might expect a more diffuse distribution of deaths throughout the year. Season of death thus provides a test of these scenarios of assemblage formation. Techniques for analyzing season of death in proboscideans and rates of tusk growth have been developed in previous work on both mastodons and mammoths (Fisher 1987, 1988, 1990, 2001; Koch *et al.* 1989; Fisher & Fox, submitted). However, this study represents the largest sample yet studied from a single time and place.

MATERIAL AND METHODS

We collected samples using a small, handheld grinder and carbide bits to excise blocks of dentin and cementum from near the proximal end of tusks that were part of the in situ display at the Mammoth Site or that had been removed during prior excavation. Sample blocks were about 4 cm transversely (normal to the tusk's long axis) by 7 cm longitudinally (parallel to the long axis), larger than minimally required so that backup sample would be available for other analyses. Blocks were positioned so that their thicker, distal margin

might yield a dentin thickness of 2-3 cm, which would likely represent more than two years of dentin apposition. We located samples to avoid conspicuous cracks that would make dentin increments harder to trace, and to yield a pulp cavity surface that was well defined and protected by *in situ* sediment. Some specimens presented relatively chalky, friable dentin, which was consolidated with cyanoacrylate at intervals during the excision process. Excision involved grinding narrow channels through cementum and dentin until reaching the sediment-filled pulp cavity. The block was then liberated by localized removal of sediment from the pulp cavity, or in cases where this was not possible, by continued channeling until a fracture could be propagated from channel to channel through the sediment. After removal of samples, the outer surface of tusks on display was restored. Sample blocks were embedded as necessary in epoxy, so that they could be held firmly during sectioning, without inducing additional damage. They were then sectioned transversely, normal to dentin increments, using a Buehler Isomet low-speed saw with a diamond wafering blade. Several 5 mm-thick slabs were cut to provide subsamples for isotope analysis and thin sections. Thin sections were produced following the protocol of Fisher (1988), with modifications discussed elsewhere (Fisher 2001). Throughout this process, tusk samples were not exposed to any aqueous medium, as rapid uptake of water by friable dentin results in severe fracturing and loss of material.

Finished thin sections were examined under a Leitz Laborlux polarizing microscope. Data on thickness and position of dentin increments were collected, using Optimas image analysis software, from linked transects crossing the thin section normal to incremental features. Circaseptan (approximately weekly) second-order features were distinguished from circadian (approximately daily) third-order features by the relative darkness and continuity of the former (Fisher 1988, 2001). Marked increments were tallied and

the software recorded their thicknesses in the direction of growth (dentin apposition). Data were then exported to a spreadsheet, where cumulative thickness was calculated to transform the record of increment thickness from the temporal domain (increment by increment, each formed at constant time intervals) to the spatial domain (mm by mm). This is critical for reconciliation of the growth increment profiles with the oxygen isotope profiles, discussed below.

During thin section production, and on the freshly completed thin sections, we noted zones of higher porosity that paralleled incremental features and that appeared darker than neighboring zones by virtue of retaining more cutting oil. Positions of inner and outer boundaries of these zones were recorded for comparison with growth increment data. In some, but not all specimens, these dark zones later disappeared as cutting oil evaporated. We have had some success stabilizing the appearance of these zones by impregnating the dentin with pigmented epoxy (Fisher 2001). Preliminary analysis of thin sections confirmed that dark, porous zones repeated on an approximately annual basis (see below), suggesting they are first-order incremental features. We used this implied estimate of rate of dentin apposition to plan the sampling design for the isotope portion of the study. Our goal was to document variation in oxygen isotope composition through about the last two years of life, achieving sub-monthly resolution during the final year and roughly monthly resolution prior to that.

Transverse block surfaces intended for isotope sampling were polished with 600-grit to remove all traces of saw marks. If circaseptan features could be followed visually on this surface, no further preparation was required, but if not, the surface was impregnated with epoxy and then polished back down to just below the original dentin level. Differential penetration by epoxy highlighted circaseptan features, making it easier to mill out isotope samples from temporally restricted zones. Polished sample blocks were mounted on car-

rier slides with the polished, transverse surface horizontal. These were then taken to a sampling stage in the Stable Isotope Laboratory of the University of Michigan Department of Geological Sciences. Under stereomicroscopic observation, the carrier slide and sample block were manually driven horizontally, relative to a vertically mounted, stationary dental drill with a 0.6 mm carbide bit. Multiple passes, following incremental features and each plunging about 1 mm into the block, were required to remove each sample. Within the penultimate year, sample spacing was at ca. 0.6 mm intervals ('full-bit'), but within the final year, spacing was at ca. 0.3 mm intervals ('half-bit'). Half-bit samples either plunge deeper into the block than full-bit samples, or run farther across it, to acquire their target mass of 20-30 mg. Samples were provenienced by recording the distance from the pulp cavity surface to the inner and outer edges of the sample path milled across the block and attributing the sample to a position midway between these. Uncollected powder was cleared from the sample block after each pass, but except for this, all material in the sampled thickness was part of one of the consecutive samples. Each sample thus includes modest time-averaging, but with no assumption that each represents an equal interval of time. Restriction of samples to zones bounded by circaseptan features means that time-averaging between successive intervals is minimal.

Oxygen isotope composition of the phosphate fraction of dentinal hydroxyapatite was measured according to the method of O'Neil *et al.* (1994), with only minor changes (Fisher and Fox, submitted). After sample dissolution, phosphate was isolated from precipitates by filtration rather than by centrifugation. Silver phosphate crystals were heated to 500°C (rather than 550°C) during degassing, and the reaction to produce CO₂ gas from silver phosphate and graphite was run at 1400°C for 1.75 minutes (rather than 1200°C for 3 minutes). The isotope composition of phosphate oxygen ($\delta^{18}\text{O}_p$) was measured in

the University of Michigan Stable Isotope Laboratory with a Finnigan MAT Delta-S isotope ratio mass spectrometer. Reproducibility of analyses reported by O'Neil *et al.* (1994) was better than 0.2‰, and we confirmed similar precision for our protocol by multiple analyses of a homogenized standard, at least one sample of which was included with each batch of dentin samples from the Mammoth Site. All analyses are listed in the Appendix.

RESULTS

Figure 1 shows the results of HS 00213, the first specimen analyzed. The $\delta^{18}\text{O}_p$ values (Fig. 1A) range from somewhat above 9‰ to almost 14‰, in a relatively simple, cyclic pattern. More important, the major excursions of this profile recur on the same spatial scale as the zones of relatively high porosity, with these zones encompassing most of each rising phase of the isotope profile. Declining phases of the profile are broader in both of the complete cycles recovered. Isotope minima, in this specimen, show no conspicuous trend through time, but the maxima in consecutive cycles decline through the three peaks recovered. Although this pattern will be replicated below, we point out that two samples, located just beyond 8 mm from the pulp cavity, were lost during the reaction (as happens sporadically, due to flaws in glass sample tubes or other causes), leaving the position of the middle peak less well constrained than would be ideal. Still, the relation of this peak to the porous zone at about 8 mm from the pulp cavity is similar to that shown by other peaks, suggesting that the apparent position of this peak has not been greatly displaced by sample loss. Death occurred just after the final peak in oxygen isotope composition, at the beginning of a declining phase of the isotope profile. Figure 1B shows a slightly smoothed (three-point moving average) version of the profile of circaseptan (second-order) increment thickness for HS 00213. Raw data for this and other specimens will be published elsewhere, as it would require more

space than is available here. However, 45-55 circaseptan incremental features were identified within each first-order couplet defined by adjacent high- and low-porosity zones, confirming this repeating pattern as annual in nature. In what appears to be the penultimate year, from about 14 mm before the pulp cavity to about 9 mm before the pulp cavity, the profile shows greater increment thicknesses associated with the rising phase of the isotope profile and the initial part of the falling phase, followed by smaller increment thicknesses associated with the rest of the falling

phase. After this point, however, the growth increment profile shows little or no clearly seasonal variation (i.e., repeating on the scale of first-order porosity features). Its mean value trends slightly upward and its variance increases. There is one conspicuous decline in tusk growth rate shortly before death, but death occurred as tusk growth rate was rising again, shortly after the end of a high-porosity zone.

Figure 2 presents, in identical fashion, results for specimen MSL 1168. Remarkably, the overall pattern is so similar that we need only mention the few points of difference.

Absolute values of the isotope profile are slightly higher, although both profiles show long runs in the vicinity of 10-11‰, late in the phase of declining values. Low increment thickness values late in the penultimate year may not be quite as marked as those of HS 00213, but they are still notable relative to the higher values from 17 to 15 mm before the pulp cavity. During the last year, increment thickness values show no obvious trend,

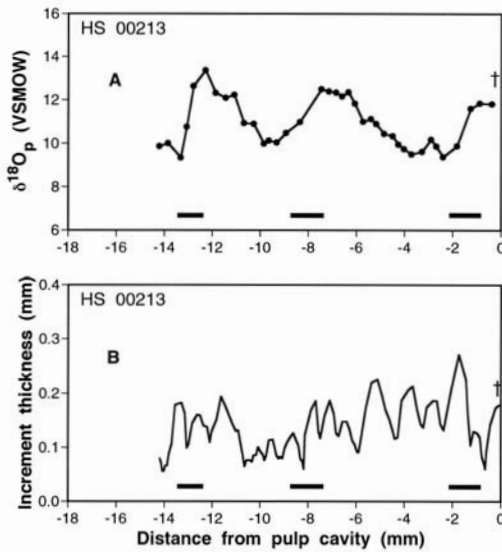


Figure 1 **A** Oxygen isotope profile for the last two-plus years of life, from tusk dentin of specimen HS 00213. Measured values of $\delta^{18}O_p$ are given relative to the Vienna-Standard Mean Ocean Water (V-SMOW) standard. Measurement error (estimated from repeated analyses of a homogeneous standard) is less than $\pm 0.2\text{‰}$ (per-mil), on the same order as the dots used to plot values. Spatial reference for consecutive samples is given as distance from the pulp cavity, increasing toward the right (in the direction of growth), toward a value of zero at death (dagger symbol at far right). Solid bars just above x-axis represent position and width of zones of increased porosity in tusk dentin. **B** Profile of variation in second-order (circaseptan) increment thickness, from tusk dentin of specimen HS 00213. Curve shown is a three-point moving average of increment thicknesses, plotted relative to cumulative thickness, and transformed to represent distance from the pulp cavity as in A. Death (dagger) and solid bars (high-porosity zones) as in A.

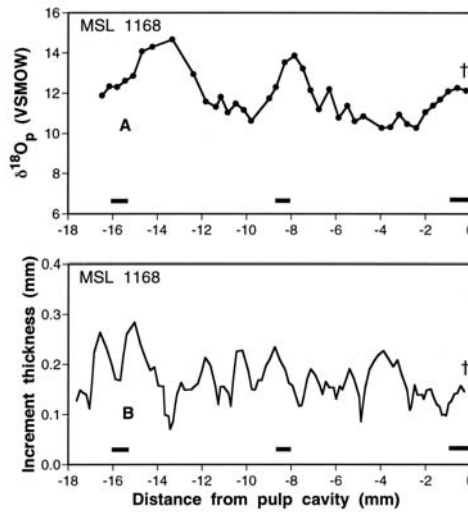


Figure 2 **A** Oxygen isotope profile for the last two-plus years of life, from tusk dentin of specimen MSL 1168. All conventions as in Figure 1. **B** Profile of variation in second-order (circaseptan) increment thickness, from tusk dentin of specimen MSL 1168. All conventions as in Figure 1.

although both years sampled in this tusk show rates of dentin apposition comparable to the higher growth rate observed during the last year of HS 00213, with total annual thickness of dentin greater than 7 mm.

Figure 3, for HS 00281, shows a similar cyclic pattern of variation in oxygen isotopes. Total range of values is similar, although absolute values are lower than for the previous specimens. In this case, both peaks and valleys of the isotope profile converge toward the end of life, with the last year again ending its declining phase near 10‰. The very last sample was lost during reaction, but the absence of any porous zone adjacent to the pulp cavity suggests that another increase in isotope value was not yet underway, and the terminal value was probably little different from that of the penultimate sample. The position of death within the annual cycle is thus notably different, occurring just after an annual minimum in oxygen isotope value, just before initiation of another high-porosity zone. The increment thickness profile shows essentially no evidence of a seasonal pattern.

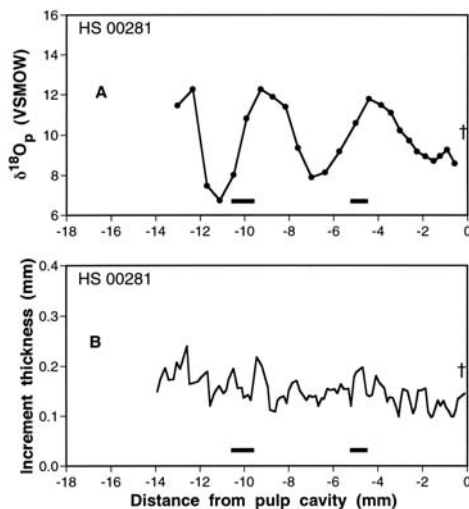


Figure 3 **A** Oxygen isotope profile for the last two-plus years of life, from tusk dentin of specimen HS 00281. All conventions as in Figure 1. **B** Profile of variation in second-order (circaseptan) increment thickness, from tusk dentin of specimen HS 00281. All conventions as in Figure 1.

Absolute rates of dentin apposition decline slightly over the years represented, but are generally on par with the shorter, penultimate year of HS 00213, at about 5 mm per year.

Figure 4, for MSL 1169, shows a smaller total thickness of dentin, and less time, because cementation of sediment filling the pulp cavity forced the sample location too far proximally for the block to transect a full two years of dentin. Still, the general form and range of values on the isotope profile is like that of other specimens. Two samples, from positions near 9 mm from the pulp cavity, were again lost in reaction, but the consistent patterns observed elsewhere suggest that these values were isotopically intermediate to the values measured on either side of those lost. As with HS 00281, death occurred just after an annual minimum in oxygen isotope value, but in this case the high-porosity zone had begun to form. No clear pattern of change in increment thickness is evident.

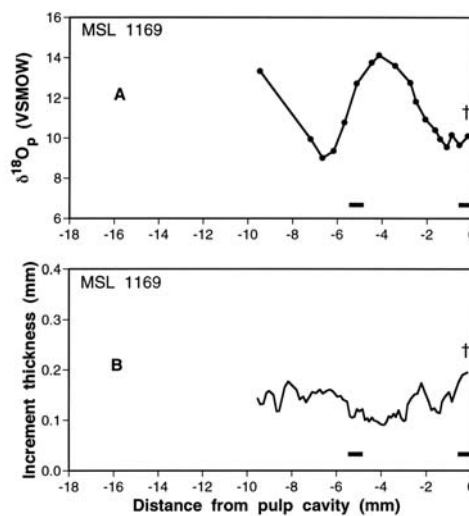


Figure 4 **A** Oxygen isotope profile for the last nearly two years of life, from tusk dentin of specimen MSL 1169. All conventions as in Figure 1. **B** Profile of variation in second-order (circaseptan) increment thickness, from tusk dentin of specimen MSL 1169. All conventions as in Figure 1.

Figure 5 shows two additional specimens for which we presently have only increment thickness profiles, supplemented by observations on the distribution of first-order porosity features. The unnumbered specimen referred to informally as ‘Stump’ (from the vertical orientation of its proximal end, the only portion yet exposed) shows a pattern of higher, then lower, increment thicknesses from 22 mm before the pulp cavity to about 15 mm before the pulp cavity, which resembles the increment thickness pattern of the penultimate years in HS 00213 (Fig. 1B) and MSL 1168 (Fig. 2B). Following this, its pattern is mostly aseasonal, although there may be some tendency for greater increment thicknesses in association with high-porosity zones and thinner increments at intermediate positions. Death occurred during production of one of the high-porosity zones. MSL 1167 (Fig. 5B) shows a penultimate year like the first observed for ‘Stump’, but little pattern, other than generally declining values, after this. Death occurred after completion of a high-porosity zone.

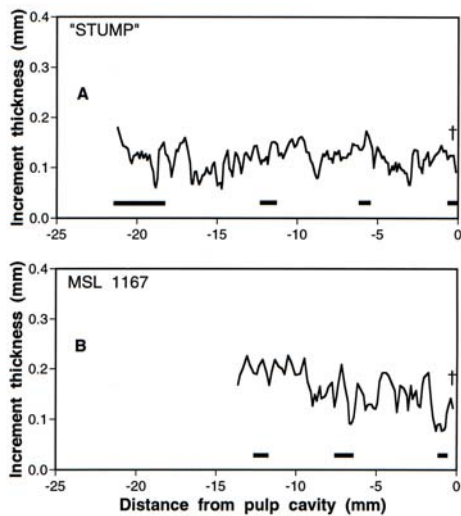


Figure 5 **A** Profile of variation in second-order (circaseptan) increment thickness, from tusk dentin of unnumbered specimen nicknamed ‘Stump’. All conventions as in Figure 1. **B** Profile of variation in second-order (circaseptan) increment thickness, from tusk dentin of specimen MSL 1167. All conventions as in Figure 1.

For three additional specimens, 89 HS 005, HS 00268, and HS 00324, we have as yet neither oxygen isotope profiles nor increment thickness profiles, but high-porosity zones can be observed on polished transverse sections. The positions of these high-porosity zones relative to the surface of the pulp cavity is similar to what was observed on HS 00213 and MSL 1168, although the high-porosity zone is slightly farther removed from the pulp cavity for HS 00324. These and other specimens will be treated in more detail in future work.

‘Beauty’

Finally, one specimen in the *in situ* display (nicknamed ‘Beauty’) presents an extended surface on the erupted, mid-portion of the right tusk, from which cementum has spalled off, revealing the topography of the dentin-cementum interface. A series of subtle, topographic annulations (transversely oriented, circumferential ridges) demarcates regular increments in tusk length. Their spacing, considering the typical angle of the appositional surface of dentin, corresponds to the expected outcrop width of first-order features in dentin thickness, such as the porosity couplets noted above. Thus the length increments are also likely first-order in nature. Indeed, their general organization matches patterns seen on many other mammoth and mastodon tusks (Fisher 1987, 1996, 2001), where topographic constriction has been related to a recurring period of seasonal nutritional stress. Successive increments to tusk length for eight consecutive years, measured where exposed, along the dorsal surface of the tusk, are: 6.0, 4.5, 3.9, 3.5, 4.0, 4.5, 3.1, and 4.1 cm. Present exposure precludes placing these years more precisely into the context of the animal’s life.

DISCUSSION

Oxygen isotope composition

The oxygen isotope profiles shown in Figures 1-4 display conspicuous cycles with ca. 4-6‰ ranges, on a 5-7 mm spatial scale. Comparable patterns have been documented previously for proboscideans (Koch *et al.* 1989, Fisher & Fox submitted), beaver (Stuart-Williams & Schwarcz 1997), and horses (Sharp & Cerling 1998), as well as sheep and bison (Fricke & O'Neil 1996). These patterns have been interpreted as recording the oxygen isotope composition of local precipitation and plant food-water, both of which are well known to vary seasonally in a manner consistent with the observed patterns. For a combination of hydrologic and physiological reasons, the typical range of variation in oxygen isotope composition of mammalian tooth tissues is lower than the range of values observed directly in local precipitation, but the ranges recorded in our study are normal for moderately seasonal, temperate climates.

Attribution of specific portions of isotope profiles to specific seasons has been treated by Koch *et al.* (1989), Stuart-Williams & Schwarcz (1997), and Fisher & Fox (submitted). Winter precipitation usually shows the lowest $\delta^{18}\text{O}_p$ values in the annual cycle, and summer precipitation the highest, but the finite time for turnover of the body-water reservoir, which is undoubtedly longer for larger mammals, tends to make the cycle in body-water composition lag behind that of precipitation. Furthermore, the lower $\delta^{18}\text{O}_p$ values of winter precipitation may not become available for mammals to drink until spring brings warmer conditions. Ultimately, the most secure basis for linking seasons to phases of the oxygen isotope profile may be to relate isotope profiles directly to growth increment profiles (Fisher 2001), as done here. In years with the clearest pattern of seasonal variation in rate of dentin apposition (discussed further below), high growth rates are typically initiated just after the isotope minimum. We thus identify the isotope mini-

mum as the winter-spring boundary. The isotope maximum marks the first evident influence of lower values in precipitation and plant-water and is interpreted as a mark of the summer-autumn boundary. These cycles each contain one high-porosity zone, generally associated with relatively high rates of dentin apposition, during the spring and summer, on the rising limb of the isotope profile.

Relationships among phenomena that vary on an annual cycle may be usefully visualized on a calendar-dial diagram such as that presented in Figure 6A. This first version shows a year with arbitrarily equal, three-month seasons, with temperature varying from a mid-summer high to a mid-winter low. As argued above, oxygen isotope composition of mammalian body water, and hence tooth tissues, though broadly correlated with the temperature signal, is shifted in phase relative to it. However, the arbitrary structure of such a year does not correspond to the patterns observed in our specimens. In particular, the declining phase of the isotope profile is broader than the rising phase. If rate of dentin apposition were constant, this observation in the spatial domain would translate directly into the temporal domain, yielding the difference in duration between spring-summer and autumn-winter. However, rate of dentin apposition is not constant, commonly falling to lower values through what we interpret as most of winter. Figure 6B has been adjusted relative to 6A to account approximately for this difference. The exact position of seasonal boundaries on such a calendar-dial would of course depend on their definitions, and for most definitions linked to local climate, would be expected to vary from year to year. Still, even a rough approximation is an improvement over arbitrarily equal seasons for plotting season of death.

Overall, the oxygen isotope profiles are the most directly informative portion of our results. Even considered in isolation, they show impressive patterns of recurrence that are strongly suggestive of annual, seasonally varying phenomena, supporting plausible

interpretations of season of death. Taken in conjunction with profiles for rate of dentin apposition, these interpretations are strongly corroborated. With respect to paleoenvironment, the isotope results imply a climate colder than at present, with moderate seasonality involving a relatively short warm season and a longer cold season.

Rate of dentin apposition

Plotting the thickness of successive circaseptan increments yields a profile of the changing rate of increase in dentin thickness (i.e., rate of dentin apposition), with approximately weekly resolution. Against this background, high-porosity zones and key features of the isotope profile tend to recur on a spatial scale that encompasses about 50 circaseptan features. The numbers of putative second-order features within putative first-order features are thus entirely consistent with the hypothesis that these represent periodically formed increments. The correspondence (at least in some of the earlier years within our samples) of profiles of rate of dentin apposition, high-porosity zones, and oxygen isotope profiles corroborates the interpretation of

annual features and confirms our ability to recognize seasons and growth patterns independently of one another. The specific combination of high porosity observed here, associated with relatively high rates of dentin apposition (again, in certain years) and rising oxygen isotope values, has not been described previously, but some pattern of first-order structural and compositional variation, with about 50 second-order features hierarchically organized within it, has been recognized as a consistent feature of tusk dentin in other mammoths (Fisher 2001; Fox 2000).

The part of this picture that was entirely unexpected prior to beginning this research was the poor correspondence between rates of dentin apposition and isotopically recognized seasons in many of the final years in the lives of these mammoths. Increment thickness profiles from other temperate region mammoths typically show much more conspicuous seasonal variation (Fisher 2001). By comparison, increment thickness profiles for Hot Springs mammoths are almost useless for determining season of death without recourse to isotopic data. The fact that certain years preceding the final

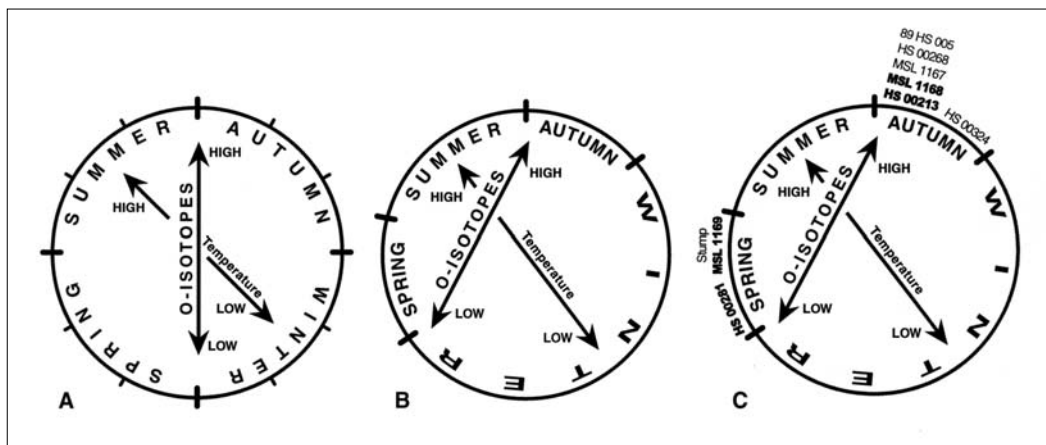


Figure 6 Calendar-dial diagrams for reporting season-of-death data. **A** Conventional portrayal of equal seasons, each with a three-month duration. Annual cycle of temperature values shows a summer high, opposite a winter low. High and low values in the cycle of variation in oxygen isotope composition are phase-shifted clockwise by a combination of body-water reservoir effects and hydrologic effects. **B** Seasonal durations adjusted to reflect time-value of the rising (spring-summer) phase and the declining (autumn-winter) phase of the cycle of variation in oxygen isotope composition. **C** Diagram from B, with season-of-death data added by specimen number: Numbers in bold represent determinations based on oxygen isotope profiles. Additional specimens (from Fig. 5 and three others) are added based on placement of high-porosity zones relative to surface of pulp cavity.

years of life sometimes show more normal patterns of seasonally varying rate of apposition suggests that the lack of clear signal in tusk growth toward the end of life is not simply a reflection of conditions that prevailed throughout this time and region. Rather, we propose that the transition from mildly seasonal to aseasonal patterns of dentin apposition reflects a change in the circumstances of life of the mammoths that ultimately were preserved at this site. This proposal is discussed below under the rubric of 'site-fidelity'.

Distribution of season of death

Applying the seasonal interpretations of Figure 6B to the isotope profiles of Figures 1A-4A yields the distribution of season of death shown by the bold specimen numbers in Figure 6C. This yields two individuals that died just after the beginning of autumn (HS 00213, MSL 1168) and two that died just after the beginning of spring (MSL 1169, HS 00281). As noted above, increment thickness profiles without isotope values are, at this site, of limited value in determining season of death, but there may be more potential for using the placement of high-porosity zones, relative to the surface of the pulp cavity. Because high-porosity zones seem to have a consistent relation to features of the isotope profile where both can be observed, they may suffice for a provisional determination of season of death. Determinations for five additional specimens have been added to Figure 6C on this basis and appear to reflect the distribution seen in the more securely determined specimens.

The pattern revealed is an annually bimodal distribution of mortality. Although it is premature to attempt any statistical evaluation of this bimodality, we can comment in a more qualitative manner. Even the non-arbitrary calendar dial of Figure 6B and C may overstate the distinction between spring, summer, and autumn. The high-porosity zones that constitute our principal point of reference for six individuals are quite variable in width, and near the surface of the pulp cavity, it is

sometimes difficult to tell whether one is looking at part of a high-porosity zone or postmortem staining related to the pulp cavity surface itself. Whether the dearth of summer deaths is as great as portrayed in Figure 6C is therefore uncertain, although we believe it represents the most likely interpretation of these data. On the other hand, deaths scattered in time throughout winter should be very conspicuous, even in data such as we have now. Their absence runs counter to both predictions mentioned in the introduction: a concentration of winter deaths and a year-round incidence of death. This reopens the issue of how mammoths were attracted to and entrapped within the Hot Springs Mammoth Site.

Evidence of site-fidelity

As indicated above, we propose that the transition from a moderately seasonal to an aseasonal profile of variation in dentin increment thickness represents a change in the lifestyle of individual mammoths. Prior to such a change, we view them as encountering more typical habitats of the high plains, with seasonally varying patterns of availability of food and water. After such a change, we view them as having consistently frequented artesian systems such as the one that produced the Mammoth Site, without necessarily having remained for long periods at any one of these. At least with respect to the type of microenvironment they came to favor, we view them as demonstrating a degree of site-fidelity. The progressively reduced ranges of oxygen isotope variation may reflect this increasing reliance on one (generic) water source, and the absolute value toward which the profiles seem to trend (ca. 10-11‰) probably reflects the composition of water derived from this source. An aquifer-fed system of this type would be expected to remain essentially invariant isotopically, with its composition reflecting only the strongly time-averaged conditions of local climate. This composition would not only dominate drinking water derived from the spring ponds and their effluents, but also the plant-water in-

gested along with vegetation growing around the pond margins or effluent watercourses. This interpretation makes the Hot Springs mammoths in certain respects a unique case, not representative of their broader temporal and geographic context, but the uniqueness of the site itself implies some degree of distinctness from a broader background. In addition, if future work probes years from even earlier in life, there will be an opportunity to clarify this distinction further.

Implications for mechanism of entrapment

It is not surprising that mammoths might show the behavioral flexibility to adapt to local patterns of resource availability and when possible, insulate themselves from seasonal shortages. This scenario is generally compatible with earlier interpretations of the mechanism of entrapment, in the sense that food and/or water are bringing the animals in from the broader environment. However, the unexpected component of this scenario is the length of time over which association with the sinkhole seems to have persisted. Furthermore, the high, or at least aseasonal, rates of dentin apposition that are sustained, if only intermittently, throughout the winters, following the onset of site-fidelity, imply that there is more to the mechanism of entrapment than just getting the animals in to eat and drink. In particular, an annually bimodal pattern of risk of mortality seems at odds with mammoths that return to an inherently dangerous site throughout the year, over periods of two years or more. Faced with this disparity, a viable interpretive scenario must explain why there are no mid-winter deaths. Given our results, we provisionally exclude the possibility that this is just sampling error.

One approach to explaining the absence of mid-winter deaths considers the potential for seasonal variation in the condition of the sinkhole margins and the consequent risk of slipping into the sinkhole itself, or the likelihood of being unable to escape. It is possible that the sinkhole margins were dry enough in

summer to present little risk and sufficiently near freezing in winter to again reduce risk. In contrast, spring and autumn may well have been wetter seasons, in which risk was on average higher and also difficult to predict. However, further consideration of such a proposal depends also on a model of the topography of the sinkhole margins and its development through time. This issue could be profitably addressed elsewhere, but takes us beyond the constraints of this study. An alternative interpretation that we view as preferable in some respects, is that the pond-margin vegetation that may have attracted mammoths to the sinkhole in spring and autumn itself died back enough in winter to reduce the likelihood of entrapment. Under this model, entrapment may be associated with essentially random events such as collapse of an oversteepened or structurally weakened bank-margin. All that is then necessary to produce the observed pattern of seasonal mortality is seasonal suspension of the attraction that brings mammoths physically to the brink of this environment. The question posed by this alternative is that if food availability in this setting was in fact low during winter (i.e., not significantly elevated relative to the surrounding landscape), what kept the mammoths 'in attendance' during the winter, as suggested by their profiles of dentin apposition?

At the risk of erecting unknown upon unknown, we offer the unsurprising proposal that water itself may be a critical and seasonally restricted resource, but we give this a different twist, appropriate for this environmental setting. Twenty-six thousand years ago, on the southern flank of the Black Hills, winter may have been the season when water was least available, not because of drought, but because of freezing. Under these conditions, a source of free water, without the thermoregulatory burden of ice or snow, may have been an extremely attractive resource. Availability of water may even have represented a constraint on somatic growth rates, not to mention rates of apposition of mineralized tissue. This may have been an especially

important factor for a large, caecal fermenter subsisting on low quality forage. The source of free water, however, need not be the sink-hole pond itself. Access to water would be safer by approaching the effluent stream. Effluent streams from this and other nearby sinkholes would be available for drinking, as well as combining into the ancestral Fall River, which would, by virtue of elevated temperature, flow longer into the cold season than other rivers in the vicinity. We thus view water as the most important factor keeping mammoths near the artesian system, and food, in spring and autumn, as the factor drawing them to high risk. Further exploration of this proposal is deferred to future work, but it has the potential to illumine some of the observations reported here.

These results leave much to be explored. However, they also offer new constraints on interpretations of site formation processes, and they enrich our understanding of the conditions of mammoth growth and survival during the time prior to the Last Glacial Maximum. Some of their most important implications will become evident only as we pursue comparative studies with mammoths from other time periods and environmental contexts (Fisher 2001).

ACKNOWLEDGEMENTS

We thank all of the directors and staff of the Hot Springs Mammoth Site for their permission to conduct this research, their long term assistance in excavating and preserving the site, and their support in collection of the samples used here. Support from NSF grant EAR 0628063 (to DCF) and Earthwatch grants (to LDA) is also gratefully acknowledged.

REFERENCES

- Agenbroad, L.D., 1994a - Geology, hydrology and excavation of the site - in: Agenbroad, L.D. & Mead, J.I. (eds.) - The Hot Spring Mammoth Site: A Decade of Field and Laboratory Research in Paleontology, Geology, and Paleoecology: 15-27, The Mammoth Site of Hot Springs, SD, Hot Springs
- Agenbroad, L.D., 1994b - Taxonomy of North American *Mammuthus* and biometrics of the Hot Springs mammoths - in: Agenbroad, L.D. & Mead, J.I. (eds.) - The Hot Spring Mammoth Site: A Decade of Field and Laboratory Research in Paleontology, Geology, and Paleoecology: 158-207, The Mammoth Site of Hot Springs, SD, Hot Springs
- Agenbroad, L.D. & Mead, J.I., 1994 - The taphonomy of *Mammuthus* remains in a closed system trap, Hot Springs Mammoth Site, South Dakota - in: Agenbroad, L.D. & Mead, J.I. (eds.) - The Hot Spring Mammoth Site: A Decade of Field and Laboratory Research in Paleontology, Geology, and Paleoecology: 283-305, The Mammoth Site of Hot Springs, SD, Hot Springs
- Fisher, D.C., 1987 - Mastodont procurement by Paleoindians of the Great Lakes Region: hunting or scavenging? - in: Nitecki, M.H. & Nitecki, D.V. (eds.) - The Evolution of Human Hunting: 309-421, Plenum Press, New York
- Fisher, D.C., 1988 - Season of death of the Hiscock mastodonts - Bulletin of the Buffalo Society of Natural Sciences 33: 115-125
- Fisher, D.C., 1990 - Age, sex, and season of death of the Grandville mastodont - Michigan Archaeologist 36: 141-160
- Fisher, D.C., 1996 - Extinction of proboscideans in North America - in: Shoshani, J. & Tassy, P. (eds.) - The Proboscidea: Evolution and Palaeoecology of Elephants and Their Relatives: 296-315, Oxford University Press, Oxford
- Fisher, D.C., 2001 - Season of death, growth rates, and life history of North American mammoths - in: West, D.L., (ed.) - Proceedings of the International Conference on Mammoth Site Studies: 121-135, University of Kansas Publications in Anthropology 22, Lawrence
- Fisher, D.C. & Fox, D.L. (submitted) - Season of death of the Dent mammoths: distinguishing single from multiple mortality events - Proceedings of the Denver Museum of Natural History
- Fox, D.L., 2000 - Growth increments in *Gomphotherium* tusks and implications for late Miocene climate change in North America - Palaeogeography, Palaeoclimatology, Palaeoecology 156: 327-348
- Fricke, H.C. & O'Neil, J.R., 1996 - Inter- and intra-tooth variation in the oxygen isotope composition of mamalian tooth enamel phosphate: implications for

- palaeoclimatological and palaeobiological research - Palaeogeography, Palaeoclimatology, Palaeoecology 126: 91-99
- Koch, P.L., Fisher, D.C. & Dettman, D.L., 1989 - Oxygen isotope variation in the tusks of extinct proboscideans: a measure of season of death and seasonality - *Geology* 17: 515-519
- Laury, R., 1994 - Paleoenvironment of the Hot Springs Mammoth Site - in: Agenbroad, L.D. & Mead, J.I. (eds.) - *The Hot Spring Mammoth Site: A Decade of Field and Laboratory Research in Paleontology, Geology, and Paleocology*: 28-67, The Mammoth Site of Hot Springs, SD, Hot Springs
- Lister, A., 1994 - Skeletal associations and bone maturation in the Hot Springs mammoths - in: Agenbroad, L.D. & Mead, J.I. (eds.) - *The Hot Spring Mammoth Site: A Decade of Field and Laboratory Research in Paleontology, Geology, and Paleocology*: 253-268, The Mammoth Site of Hot Springs, SD, Hot Springs
- Lister, A. & Agenbroad, L.D., 1994 - Gender determination of the Hot Springs mammoths - in: Agenbroad, L.D. & Mead, J.I. (eds.) - *The Hot Spring Mammoth Site: A Decade of Field and Laboratory Research in Paleontology, Geology, and Paleocology*: 208-214, The Mammoth Site of Hot Springs, SD, Hot Springs
- O'Neil, J.R., Roe, L.J., Reinhard, E. & Blake, R.E., 1994 - A rapid and precise method of oxygen isotope analysis of biogenic phosphate - *Israel Journal of Earth Science* 43: 203-212
- Sikes, S.K., 1971 - *The Natural History of the African Elephant* - Weidenfeld & Nicolson, London
- Sharp, Z.D. & Cerling, T.E., 1998 - Fossil isotope records of seasonal climate and ecology: straight from the horse's mouth - *Geology* 26: 219-222
- Stuart-Williams, H.LeQ. & Schwarcz, H.P., 1997 - Oxygen isotopic determination of climatic variation using phosphate from beaver bone, tooth enamel, and dentine - *Geochimica et Cosmochimica Acta* 61 (12): 2539-2550

received 30 June 1999

APPENDIX

Results of oxygen isotope analyses, by sample number and distance from the pulp cavity, are listed below (VSMOW, Vienna Standard Mean Ocean Water; —, sample lost during reaction).

Specimen	Sample	Distance (mm)	$^{18}\text{O}_\text{p}$ (VSMOW)	Specimen	Sample	Distance (mm)	$^{18}\text{O}_\text{p}$ (VSMOW)
HS 00213	-1	-0.38	11.8	MSL 1168	-1	-0.18	12.1
	-2	-0.88	11.8		-2	-0.57	12.3
	-3	-1.25	11.6		-3	-0.98	12.1
	-4	-1.56	—		-4	-1.33	11.7
	-5	-1.82	9.9		-5	-1.64	11.4
	-6	-2.40	9.4		-6	-1.99	11.1
	-7	-2.68	9.9		-7	-2.40	10.3
	-8	-2.90	10.2		-8	-2.80	10.5
	-9	-3.26	9.6		-9	-3.16	10.9
	-10	-3.70	9.5		-10	-3.55	10.3
	-11	-4.01	9.8		-11	-3.94	10.3
	-12	-4.25	9.9		-12	-4.33	—
	-13	-4.49	10.3		-13	-4.75	10.9
	-14	-4.85	10.4		-14	-5.14	10.6
	-15	-5.17	10.9		-15	-5.48	11.4
	-16	-5.40	11.1		-16	-5.87	10.8
	-17	-5.72	11.0		-17	-6.29	12.2
	-18	-6.06	11.8		-18	-6.75	11.2
	-19	-6.33	12.3		-19	-7.13	12.1

APPENDIX (continued)

Results of oxygen isotope analyses, by sample number and distance from the pulp cavity, are listed below (VSMOW, Vienna Standard Mean Ocean Water; —, sample lost during reaction).

	-20	-6.60	12.2		-20	-7.47	13.2
	-21	-6.85	12.3		-21	-7.85	13.9
	-22	-7.15	12.4		-22	-8.28	13.5
	-23	-7.46	12.5		-23	-8.67	12.3
	-24	-7.79	—		-24	-8.97	11.7
	-25	-8.34	11.0		-25	-9.38	—
	-26	-8.92	10.5		-26	-9.79	10.6
	-27	-9.32	10.0		-27	-10.12	11.2
	-28	-9.64	10.1		-28	-10.47	11.5
	-29	-9.85	10.0		-29	-10.84	11.0
	-30	-10.26	10.9		-30	-11.15	11.8
	-31	-10.68	10.9		-31	-11.37	11.3
	-32	-11.08	12.2		-32	-11.82	11.6
	-33	-11.44	12.1		-33	-12.38	12.9
	-34	-11.86	12.3		-34	-12.83	—
	-35	-12.28	13.4		-35	-13.33	14.7
	-36	-12.79	12.6		-36	-13.76	—
	-37	-13.06	10.7		-37	-14.23	14.3
	-38	-13.32	9.3		-38	-14.70	14.1
	-39	-13.84	10.0		-39	-15.09	12.8
	-40	-14.20	9.9		-40	-15.45	12.6
HS 00281	-1	-0.21	—		-41	-15.80	12.3

APPENDIX (continued)

Results of oxygen isotope analyses, by sample number and distance from the pulp cavity, are listed below (VSMOW, Vienna Standard Mean Ocean Water; —, sample lost during reaction).

-2	-0.57	8.6		-42	-16.15	12.3
-3	-0.91	9.3		-43	-16.48	11.9
-4	-1.22	8.9	MSL 1169	-1	-0.17	10.1
-5	-1.5	8.7		-2	-0.54	9.7
-6	-1.87	8.9		-3	-0.89	10.2
-7	-2.25	9.2		-4	-1.11	9.6
-8	-2.59	9.7		-5	-1.40	10.0
-9	-3.01	10.2		-6	-1.62	10.4
-10	-3.42	11.1		-7	-2.06	10.9
-11	-3.86	11.5		-8	-2.48	11.8
-12	-4.4	11.8		-9	-2.74	12.8
-13	-5	10.6		-10	-3.40	13.6
-14	-5.73	9.2		-11	-3.78	—
-15	-6.37	8.1		-12	-4.12	14.1
-16	-6.99	7.9		-13	-4.45	13.8
-17	-7.59	9.4		-14	-5.13	12.7
-18	-8.16	11.4		-15	-5.67	10.8
-19	-8.73	11.9		-16	-6.15	9.4
-20	-9.27	12.3		-17	-6.65	9.0
-21	-9.9	10.8		-18	-7.19	10.0
-22	-10.49	8.0		-19	-7.76	—
-23	-11.11	6.7		-20	-8.30	—

APPENDIX (continued)

Results of oxygen isotope analyses, by sample number and distance from the pulp cavity, are listed below (VSMOW, Vienna Standard Mean Ocean Water; —, sample lost during reaction).

-25	-12.33	12.3	-22	-9.46	13.3
-26	-13.01	11.5			

DEINSEA - ANNUAL OF THE NATURAL HISTORY MUSEUM ROTTERDAM
P.O.Box 23452, NL-3001 KL Rotterdam The Netherlands